IDEA PROJECT FINAL REPORT
Contract ITS-24

IDEA Program
Transportation Research Board
National Research Council

January 15, 1996

Passive Optical Lane Position Monitor

Joseph M. Geary
Swales and Associates, Inc.

INNOVATIONS DESERVING EXPLORATORY ANALYSIS (IDEA) PROGRAMS MANAGED BY THE TRANSPORTATION RESEARCH BOARD (TRB)

TABLE OF CONTENTS

1. EXECUTIVE SUMMARY

Any implementation of a lane position monitor should incorporate virtues such as simplicity, compactness, ruggedness, and low cost. The optical lane position monitor discussed here embodies these qualities to a large extent. The novel and innovative sensor head shown in **Figure 1.1(a)** consists of a cylindrical lens and a position sensitive detector. It is envisioned that this small package would be mounted on the windshield inside the vehicle up behind the rearview mirror. It would view the roadway about 15-20 feet ahead of the vehicle. (The amplifier and processing electronics would be about the size of a cigarette pack and located elsewhere in the vehicle.) This is a passive sensor which relies on available light and current road marking practice. There are no moving parts.
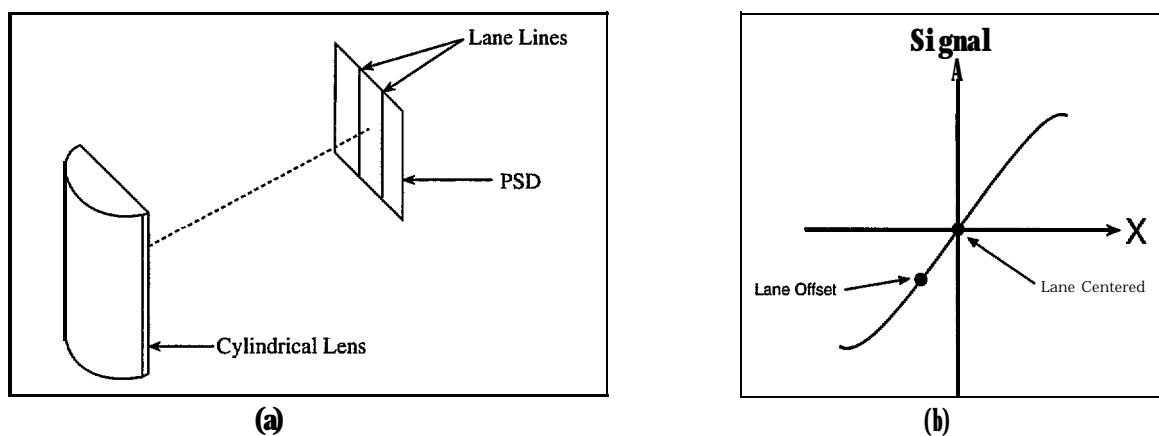
Figure 1.1 Passive optical lane position monitor.

When oriented parallel to the lane, the cylindrical lens will only image lane lines as lines. These lane lines are imaged onto a position sensitive detector. The lateral location of the lane image is directly sensed by this detector. It generates a signal linearly related to the lateral offset of the lane centroid as illustrated in **Figure 1.1(b).** Note that no computer or image processing is needed, nor software required.

A prototype of the lane position monitor described above was designed, built, and tested. This project empirically validated sensor performance both in the laboratory and in the field. The prototype was successfully tested in sunlight over a range of solar angles from dawn to dusk. It was even tested at night with the lane illuminated by a car's headlights. The bottom line is that, for such a simple system, the sensor worked quite well. This opens up exciting possibilities for its use as a practical tool in highway applications.

2. IDEA PRODUCT

A prototype passive optical lane position monitor has been designed, built, and successfully tested. The sensor head is simple and consists of two parts: a cylindrical lens, and a position sensitive detector. The amplifier/processing electronics which provides the position signal is compact and lightweight. No complex software or computer is needed. This lane position monitor is quite different from anything previously reported, and because of its simplicity, appears more practical.

This lane position monitor has a number of potential applications. First, it could be used as a diagnostic tool to measure a driver's steering control under a variety of road and lighting conditions. Second, it could be used to assess driver performance under impediments such as drowsiness or intoxication. Third, it could be coupled to an alarm to warn a driver when he is unintentionally drifting out of his lane. This may find immediate application in tractor-trailer vehicles . Fourth, it can provide the basic sensor in an automated steering system in a "smart car" scenario.

3. CONCEPT AND INNOVATION

The sensor described in this report takes two established technologies and unites them in a new and novel way to form a passive optical lane position monitor. The resulting monitor is simple, compact, rugged, and cost effective. This is a passive sensor which relies on available light and current road marking practice. It has no moving parts. Part of the monitor's simplicity is that no computer (with associated complex software) is needed. The sensor head consists of a cylindrical lens and a position sensitive detector. Both components have long independent histories, The innovation is the marriage of the two for the mission of sensing position within a highway lane.

A cylindrical lens forms a line image of a point source parallel to the cylinder axis illustrated in **Figure 3.1(a).** A line object parallel to this axis will also be imaged as a line parallel to the cylinder axis as shown in **Figure 3.1(b).** Since lane markings are lines, the cylindrical lens enhances or reinforces the imagery of such objects. The lane image will be two parallel lines.

(a)

(b)
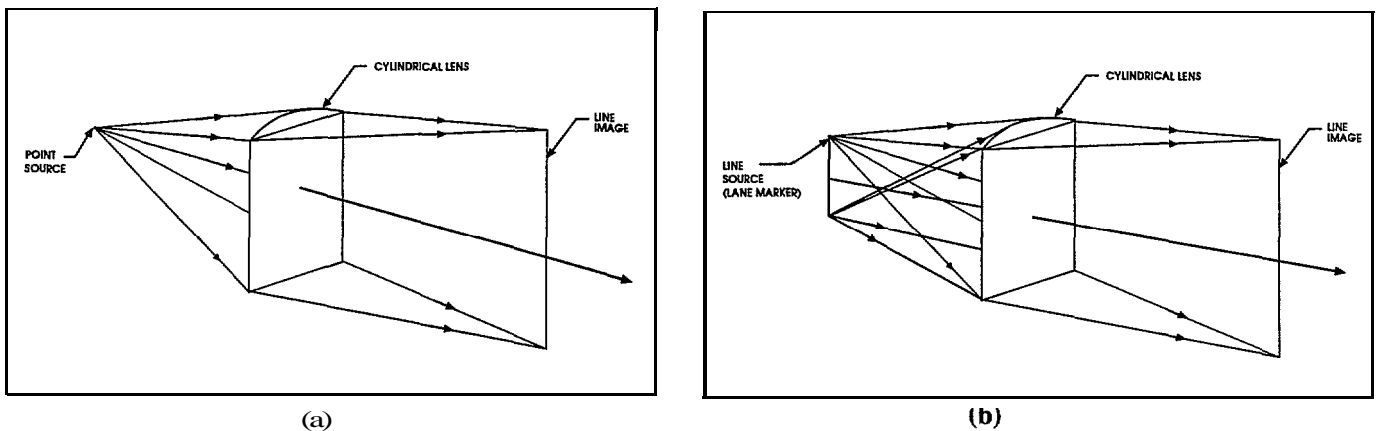
Figure 3.1 Images formed by a cylindrical lens.

The lateral location of the lane image formed by the cylindrical lens is measured with a position sensitive detector. This detector chip is a single Si crystal photopot. As the lane image shifts laterally across the detector chip (as illustrated in **Figure 3.2),** a voltage is generated which is directly proportional to the image centroid location. This position signal is independent of power level or power fluctuations in the incident light (because the signals are normalized against total power). A generic plot of this signal vs the lateral position of the lane is illustrated in **Figure 3.3.**
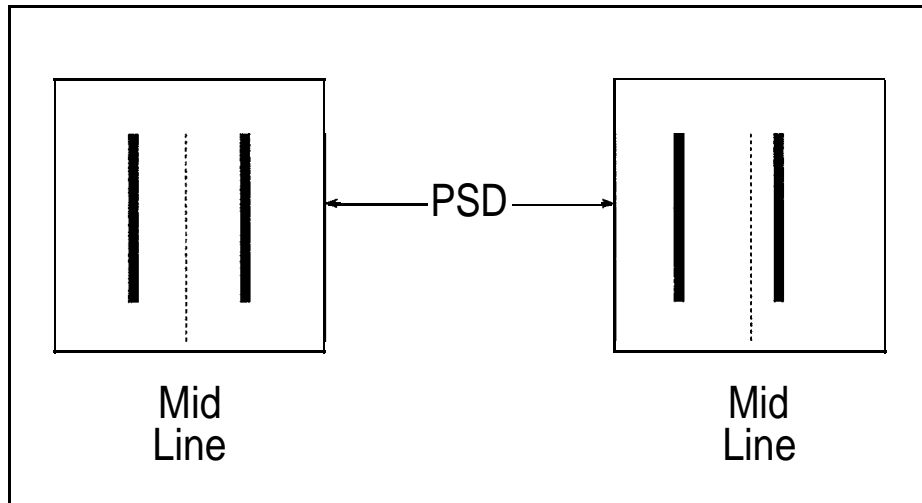
Figure 3.2 Optical lane position monitor concept.
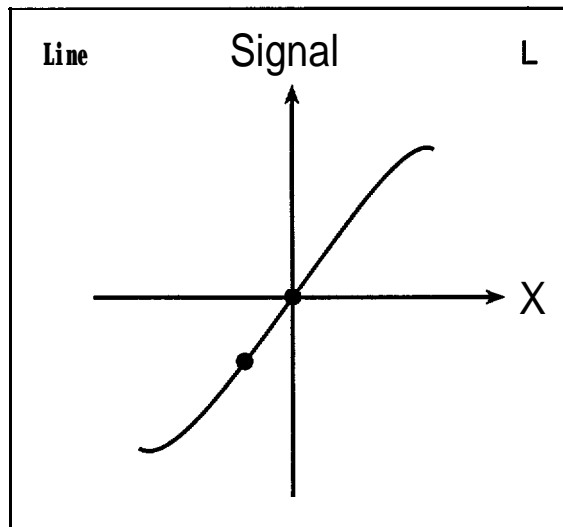
Figure 3.3 Operational principle of a PSD.

4 . INVESTIGATION

4.1. Introduction

The work discussed in this report is primarily experimental. The goal was to empirically determine whether a lane position monitor (LPM) based on a sensor head consisting of a cylindrical lens coupled to a position sensitive detector (PSD) would actually work, and under what conditions it would do so. The effort was divided into both laboratory and field tests. The former helped define the performance of the LPM under ideal and controlled conditions, and also provided benchmark data against which field results could be compared. The field experiments provided more realistic lighting conditions and operational geometries. There were two main laboratory configurations (Lab I and Lab II) and two distinct field configurations (Field I and Field II). The principal kinds of data collected from these experiments were radiometric profile scans, position scans, and photographic recordings of the lane image.

Lab I employed an on-axis optical arrangement which was used to obtain: a) relative radiometric measurements of image line structure (to see the impact of lens aberration over the operational field of view as a function of focus); b) lateral scans across a stationary lane image with the PSD (to establish baseline LPM characteristic curves as a function of focus); c) lateral scans of the lane image across the PSD by lateral motion of the source (to mimic the actual operational mode of a vehicle moving side-to-side within a lane); d) behavior of the LPM characteristic curve to glare light (contrast change), reflected light, broken lane lines, line color changes, and weak signals; e) image behavior in the presence of a clocking error between the cylindrical lens and the lane object. Lab II employed an off-axis test configuration in both elevation and azimuth angles. It had a shorter focal length cylindrical lens and a wider field-of-view. Lab II was used to obtain more realistic data on LPM sensor behavior using a geometry approximating an operational scenario.

The Field I setup used the same test stand and sensor head employed in Lab II. Now, however, the source object was an actual lane illuminated by the Sun. Data was collected under different solar illumination conditions. The Field II test configuration attached the Lab II sensor head on a minivan for static tests in the parking lot.

Because of the diverse and extensive nature of the tests performed on the LPM a great deal of data has been collected. The equipment used to do so was available in-house from the Swales optics laboratory. No equipment was purchased with project funds.

4.2 Lab I Description

The breadboard configuration used to test the basic LPM concept is illustrated in **Figure 4.1.** The lane simulator is shown on the left. It consists of a lamphouse containing an incandescent lamp, opal diffuser, and lane mask. The lane mask is a thin 2" square plate with two parallel slits 45 mm long by 1 mm wide separated by 1". An additional thin tape diffuser is attached to the back of this mask. The two diffusers assure the uniform brightness of the lanes. The front side of the mask is painted matte black.
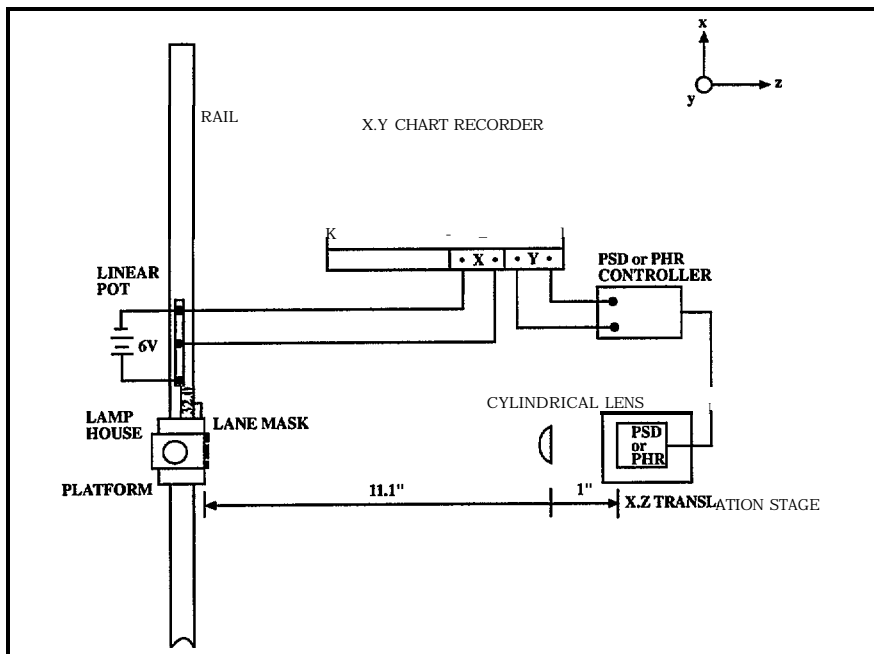
Figure 4.1 Lab I test configuration.

The overall brightness of the lanes is controllable via a Variac. This feature is useful for determining the behavior of the LPM over a range of illumination (or signal) levels. Contrast changes between lane lines (due to a broken or segmented lane line) can be accommodated by the insertion of a Wratten neutral density filter behind one slit of the lane mask. The lamphouse sits on a rail which allows lateral motion. Attached to the supporting platform is a linear potentiometer with a 7.5 cm travel range. The output of this pot can be connected to the X-axis of an XY chart recorder. Moving the lamphouse will simulate motion of the LPM (or vehicle) within a lane.

The LPM sensor head is on the right in Figure 4.1. It consists of a Melles-Griot cylindrical lens (f=l") and a PSD. The PSD is a single crystal photopot with a 1 cm square chip (from Graseby Optronics). The PSD is mounted so that it has both X and Z degrees of motion freedom. The X-motion is contolled by a motor-driven lateral translation stage. The Z-motion is contolled manually via a micrometer on an axial translation stage. This allows the focus position of the PSD to be varied. The position signal from the PSD processing electronics (301-DIV amplifier) is used to drive the Y-axis of the chart recorder. When the PSD is being scanned through the line pair image, the X-axis of the recorder runs on its internal time base . If one faces the PSD during a scan, the PSD moves left to right. (Note: These scans were generally made in a darkened room with light baffles around both the target and sensor head.)

The PSD can be replaced with a pinhole radiometer (PHR) to scan the line images formed by the cylindrical lens. The radiometer used was the IL1700 from International Light. The detector head was a SED(033) with a 5.7 millimeter square Si chip. A pinhole 100 microns in diameter was attached and centered on the detector head. Like the PSD scans, all PHR scans are made left to right.

The PSD can also be replaced with a Polaroid camera-back to record the line images on photographic film. This is useful to provide a visual record of what the PSD and PHR see during their scans. This record is also useful in obtaining dimensional measurements of the line images.

4.3 Lab I Test Results

4.3.1 PHR Scans

Due to aberration in the cylindrical lens, the image of a single lane line changes its irradiance profile as the lamphouse is swept laterally over the full field of view. Furthermore, this profile also depends on focus setting. The reason for measuring the line spread function under these different conditions is a precaution in the event that power redistribution influences the quality of the PSD scans.

Figure 4.2 is a montage of lane line profiles as a function of lamphouse lateral offset and PHR focus shift. The middle row is set at best visual focus. The top row is 2 mm inside focus. The bottom row is 2 mm outside focus. Note the striking differences in shape between the three on-axis focus cases. The lamphouse is shifted from the on-axis case laterally over a range of ± 3 cm at half centimeter intervals (which is equivalent to a $\pm 6^{o}$ field angle).

In any row one can see that there is mirror symmetry between profiles equidistant from its respective on-axis case, i.e. the shapes for equal lateral offsets are about the same but flipped 180". One can see that the on-axis line scans are symmetric, but that this symmetry continually degrades as the lateral off
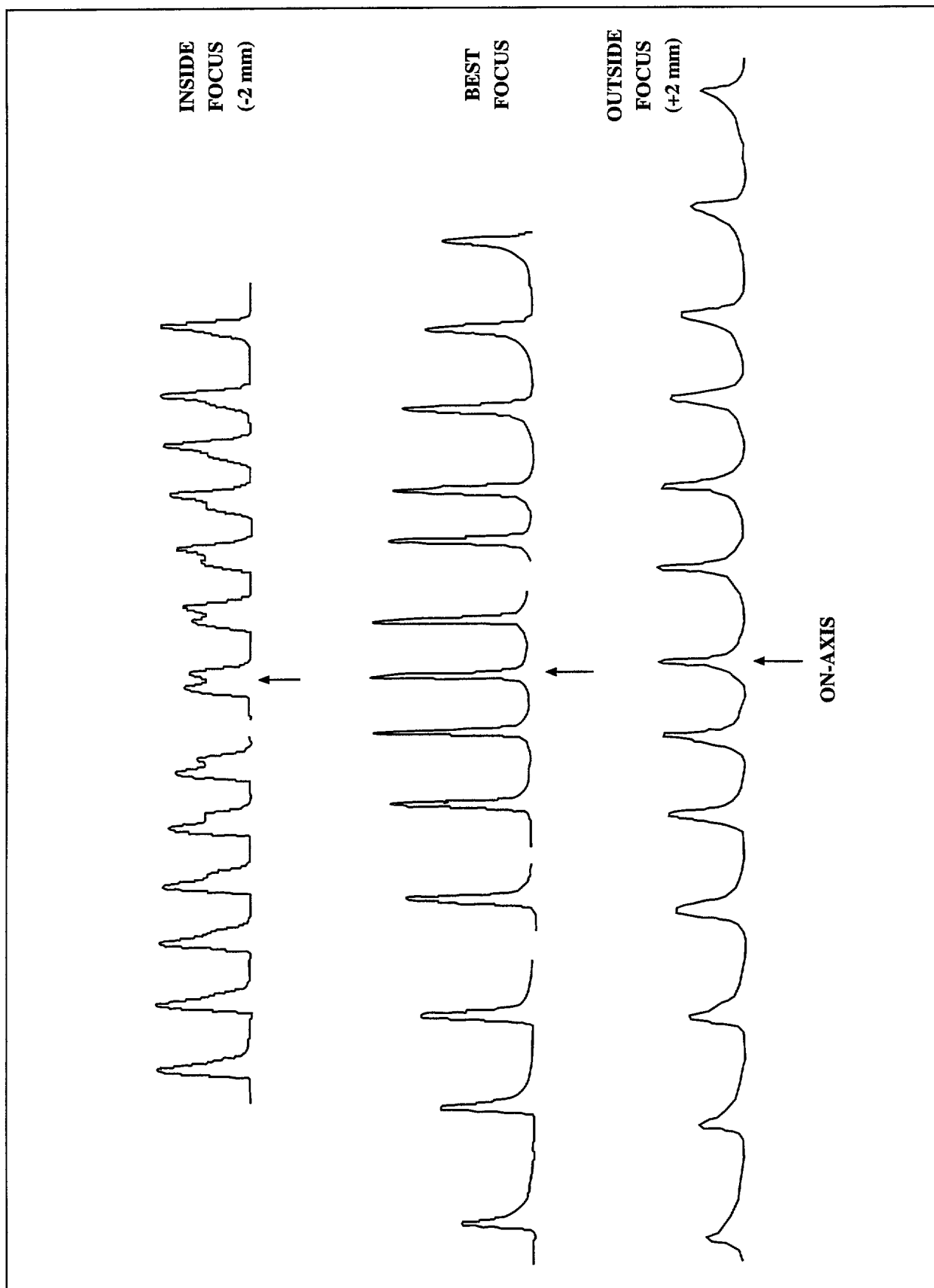
Figure 4.2 PHR scans of single lane line as a function of lateral offset and focus.

set increases. The line widths also increase. The peak powers drop on either side of the on-axis position for the best, and outside focus cases.For the inside focus case (top row), the on-axis power has a double peak which is lower than any off-axis peak power. The inside focus case also has more sharply defined boundaries. Low irradiance wings are evident in both the best and outside focus cases.

When the lane mask is centered on-axis, the two lane lines reside off-axis by ±12.7 mm. **Figure 4.3(a-c)** show profile scans for the lane pair as a function of focus when the pair are centered with respect to the optical axis of the cylindrical lens. They are arranged as follows: a) inside focus; b) best focus; c) outside focus. **Figure 4.4** shows the corresponding photograph for the best focus position.
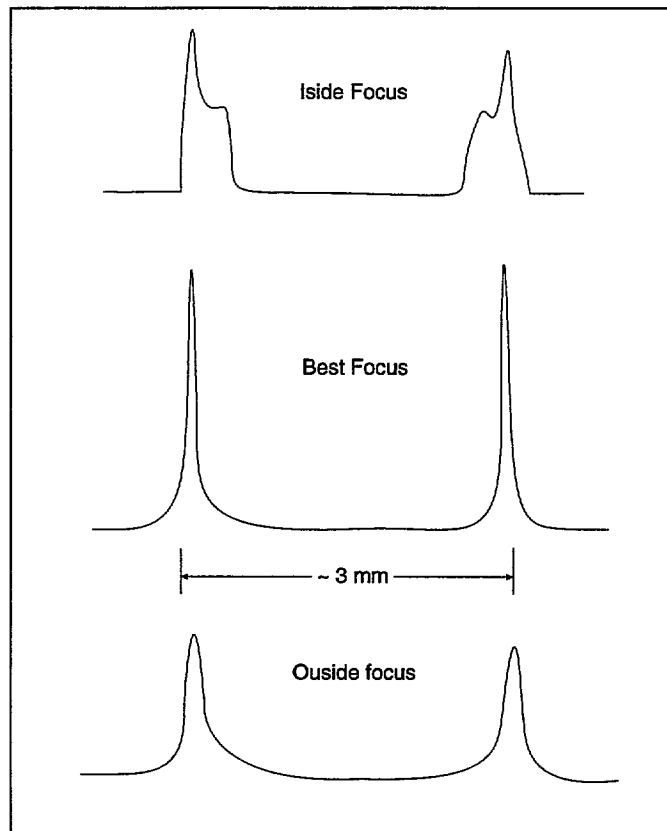
Figure 4.3 PHR scans across a centered lane image as a function of focus.

7
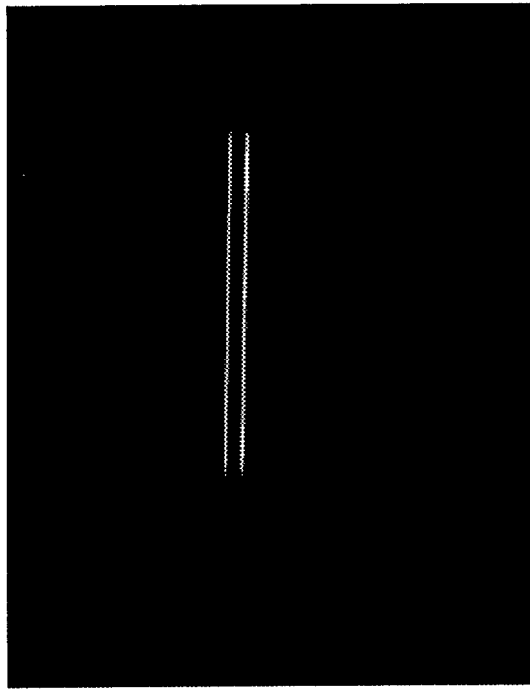
Figure 4.4 Photograph obtained in cylindrical lens image plane at best focus.

4.3.2 PSD Scans (Detector)

For these data plots made with the PSD, the detector chip was scanned through the stationary image of the lanes. There is no direct connection between the position of the X-axis translator on which the PSD rests and the X-axis of the chart recorder. For these scans the latter is driven by the internal time base (2 mm/sec) of the chart recorder. It is assumed that both the motor-driven translation stage and the X-axis motion of the recorder are uniform. Both motions are manually initiated simultaneously. For the Y-axis signal, the 301-DIV gain is set at 1M.

Figure 4.5 shows the position scan signal from the PSD as the latter is scanned across the best focus location of the lane image. The central linear region of the plot is where both lane lines are imaged on the detector chip. The X-axis range is ±4.2 mm; the Y-axis, ±4.5 volts. The linear offset portions at either end of this range are where a single lane line is imaged onto the chip. The slight scalloping seen in the linear portion of the curves is due to some minor wobbling in the motorized translation stage. The effects of a ±2 mm focus offset on PSD plots were not significant.
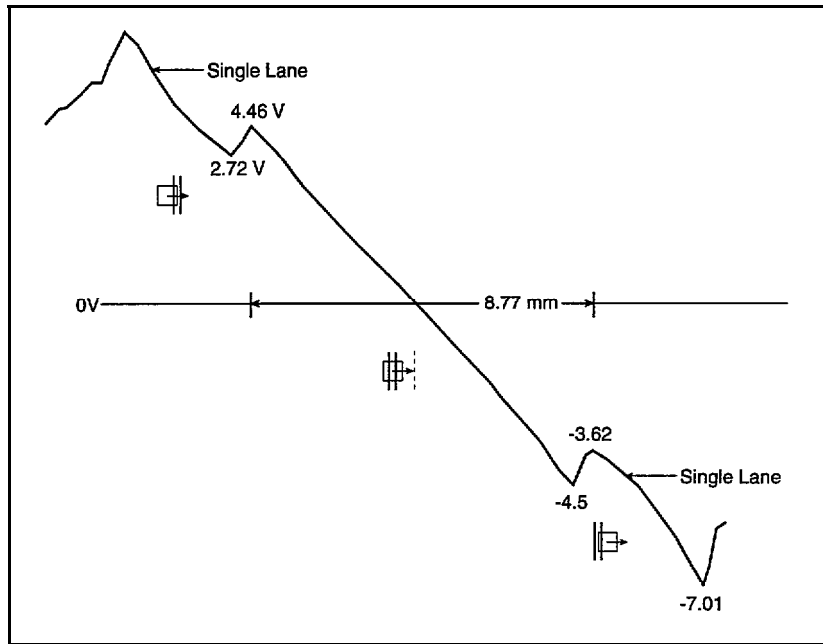
Figure 4.5 PSD detector scan of lane image at best focus.

When driving on real roads the lane line marking pattern is not always the same on either side. For example, what happens to the PSD characteristic curve when one lane line is solid but the other is broken (50% duty cycle)? Let's use **Figure 4.6(a)** to illustrate what to expect. The solid characteristic curve shows what happens when both lane lines have identical power. The curve passes through zero when the lane image is perfectly centered on the PSD detector chip. With the lane lines still centered, let the power increase in the left hand lane line. Although nothing has moved, the PSD will interpret this as a lateral shift of the lane. There will be a non-zero voltage signal out of the PSD. The new plot of the characteristic curve will be shifted vertically relative to the baseline plot, but have the same slope.
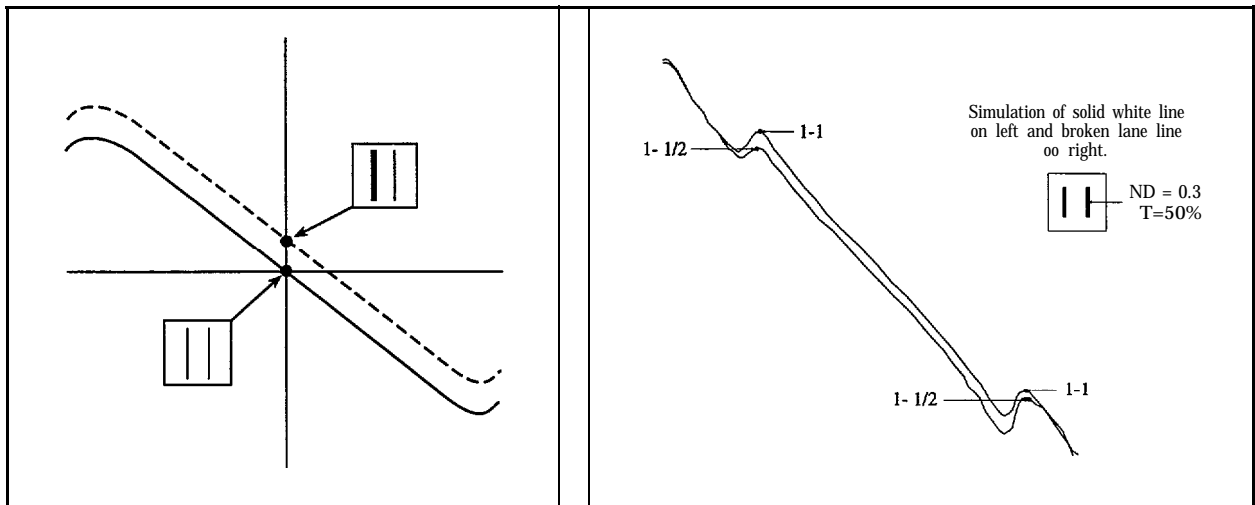
(a)   (b)

Figure 4.6 The effect of a broken lane line on the PSD detector scan: a) theoretical; b) experimental.

To address this question experimentally, return to the standard test setup shown in Figure 4.1. A broken lane line can be simulated with a 0.3 neutral density filter inserted behind the right hand target slit. This will cut the intensity from this lane line in half. **Figure 4.6(b)** shows the PSD scan of the lane image for equal lane line powers, and when one is down by 50%. The numbering "l-l" indicates the equi-power lane lines; "l-l/2", the unequal case. As expected, the characteristic curve maintains the same slope but there is a vertical shift between the two cases.

4.3.3 PSD Scan (Source)

In real life use the PSD will be stationary while the image of the lane lines move relative to the chip (due to vehicle lateral motion within the lane). However, the data collected in the previous sections represents an ideal against which comparisons can be made. The irradiance structure of the line image was fixed during a position scan. When the source moves instead of the PSD this will no longer be true (as was seen by the PHR data in **Figure 4.2).**

A source scan position plot at best focus is shown in **Figure** 4.7. The total range of travel is about 7.3 cm. The relative position of the lane pair image on the chip is indicated at the travel extremes. Note that the wobble seen previously in the PSD scans is absent here. Overall, the plot is fairly linear over the central 6 cm of travel. This means that the changing h-radiance structure in the line images as a function of lateral offset is not causing any significant degradation in the performance of the LPM sensor head.
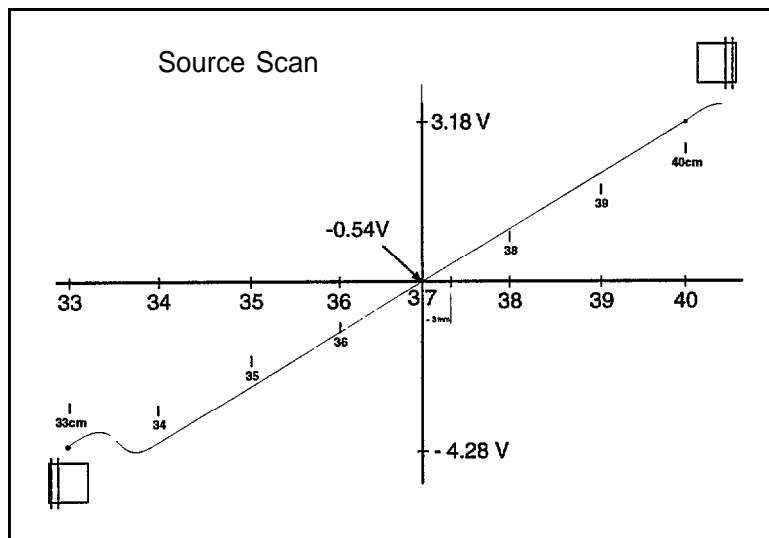
Figure 4.7 PSD source scan of lane image at best focus.

4.3.4 Effect of Reduced Lane Signal

Recall that the lane target radiance can be varied because the lamphouse is plugged into the Variac. This controls the power getting to the lamp and, hence, its light output. Ideally, changing the radiance of the lane should have no effect on the PSD signal output because the latter is normalized by total power on

the chip. **Table 4.1** shows the Variac settings and the corresponding lamp output in lumens/cm^2 as measured at the cylindrical lens plane. Note that the relationship between Variac setting and the resulting illumination is nonlinear. For example, a 50% setting cuts the light by l/23 instead of l/2. (Settings below 40% were not used because of the large amount of noise induced on the chart pen Y-axis signal.) Overall the illurninance was varied almost two orders of magnitude.

<div align="center">

TABLE 4.1

</div>

Variac Setting	Illuminance	Normalized Illuminance
100%	6.38 X 10^4	1 .000
75%	1.94 x 10"	0.304
50%	2.74 X 10^5	0.043
40%	7.56 X 10^{-6}	0.012

The effect on the PSD characteristic curve is shown in **Figure** 4.8. Note that the plots are linear over the region of interest for all cases. As illuminance is initially decreased, there is virtually no change in the PSD slope. When the illuminance is down by a factor of 23, the slope has decreased slightly. However, the slope remains stable thereafter even when the illuminance is down by a factor of 83. The change in slope is likely related to the "low lite" warning on the 301-DIV (which was on during the entire scan for the latter **two** cases)

<div align="center">
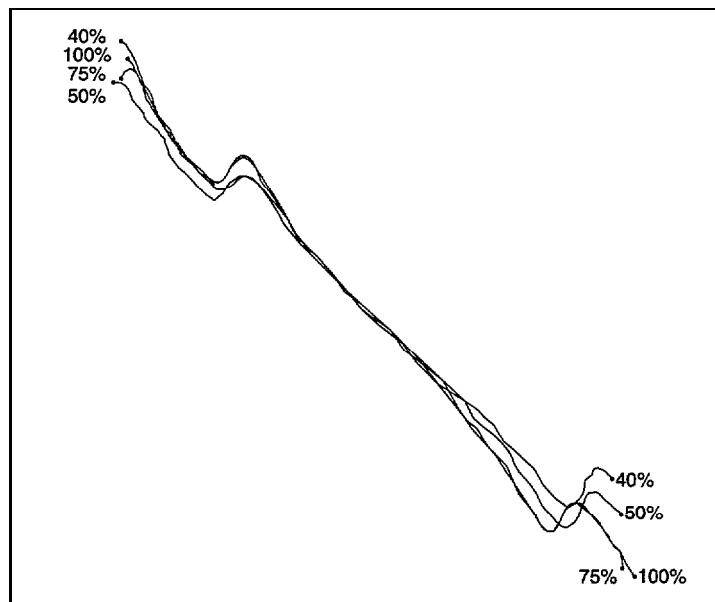
Figure 4.8 PSD behavior as radiance of lane is varied.

</div>

4.3.5 Effect of Background Changes

The output signal of the PSD is supposedly independent of changes in background illumination because the position signal is normalized against total power. The proviso is that the h-radiance distribution is uniform (or at least bi-symmetric). To generate a variable background, the Lab I test configuration was modified in the following manner. Between the target lamphouse and the LPM sensor head a beam

splitter (BS) was inserted at 45° . The BS is 3" from the target. A ground glass (diffuser) screen is placed 3" from the BS in the orthogonal direction. This diffuser screen is also back-illuminated by a Leica projection lamp. It illuminates a circle on the screen 2.6 inches in diameter. **Figure 4.9** shows the modified test configuration.
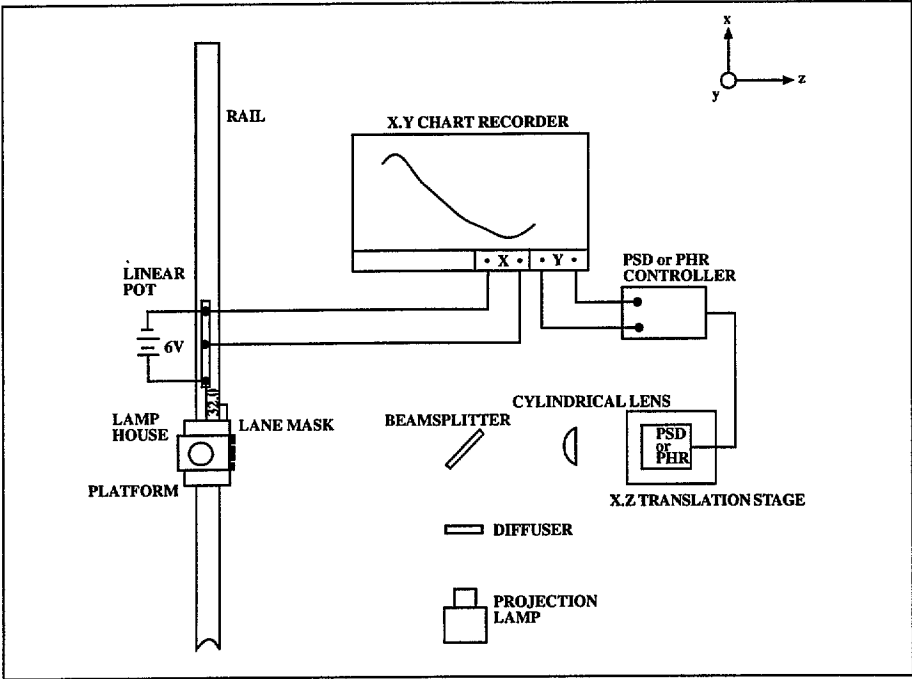
Figure 4.9 Lab I modified for variable background illumination.

Pinhole radiometer (PHR) scans were made across the lane image for four different settings of the background illumination. These profiles are shown in **Figure 4.10(a-d)**. In **(a)** there is no background light. **Figures (b-d)** show increasing levels of background illumination (with a corresponding decrease in target 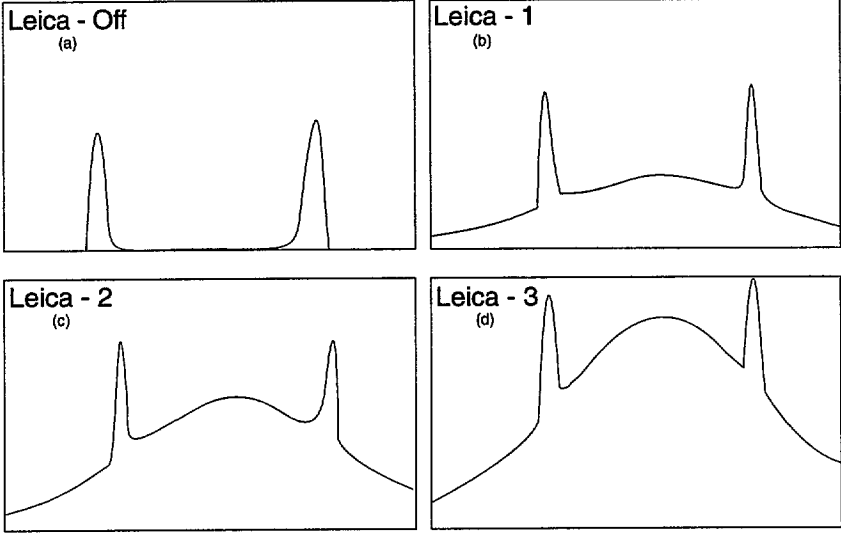contrast). Note that the background illumination in the image plane is not uniform but gaussian-like in appearance, and that its peak is not quite centered within the lane image. The latter will introduce a slight offset bias in the PSD plot (since the PSD senses the centroid of power).

Figure 4.10 PHR scans of target image with variable background.

PSD detector scans for all four cases are shown in **Figure 4.11.** The "no background" plot shows the distinctive notches when each of the lane lines transits off the detector chip. When the background illumination is turned on, these notches are washed-out. There is a slight change in slope between the on and off cases, and a slight vertical displacement of the "background on" curves (due to the lack of centration between the lane lines and the background peak). (Note: The gain setting on the 301-DIV amplifier was changed from 1M to 100K between the "background off" case and the "background on" cases because of the increased light level on the detector.)

The three "background on" plots are essentially coincident despite the significant changes in light levels. This shows that the PSD is indeed independent of background illumination changes as was expected. However, the plots in Figure 4.11 also point to a potential problem. The lost of detail seen in the PSD plot when the background illumination was turned on suggests that significant background light could overwhelm the lane signal. In real life the lane image would move relative to a stationary background signal. But if this background is too strong, lane image movement on the PSD chip might generate a plot with a very shallow slope too shallow to be useful. This question can be addressed only in a test setup which allows lane image motion against a stationary background. Such a configuration is discussed in the next section.
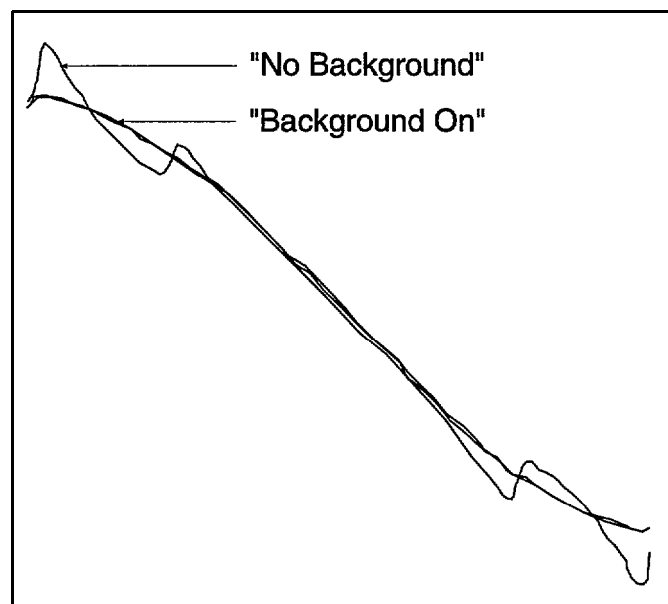
Figure 4.11 Effect of variable background illumination on PSD characteristic curve.

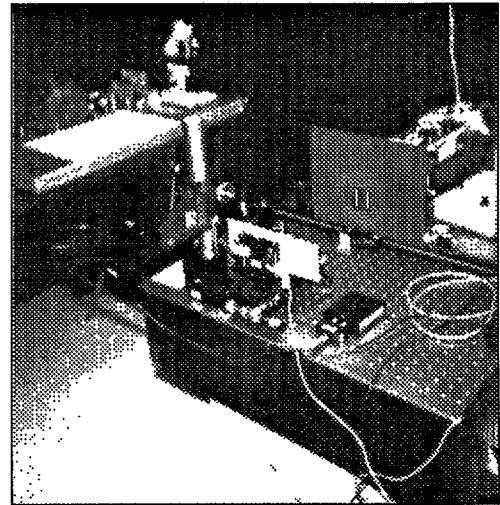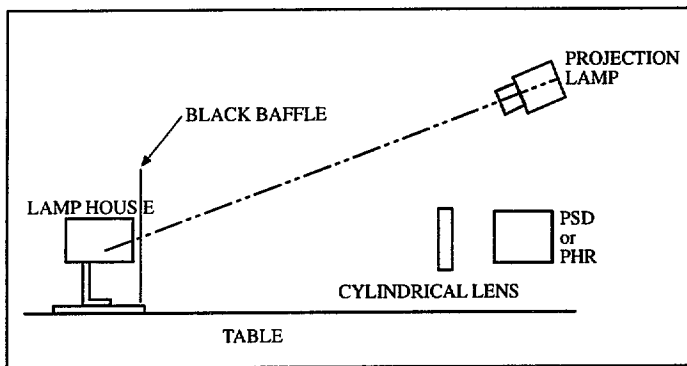**4.4 Lab I Modification For Reflected Light.**

The lamphouse configuration discussed in Sec.4.2 is based on light transmission . This transrnissive setup provides ideal high contrast lanes, and will provide the best signal to the LPM. Actual highway lanes are viewed with reflected light. Contrast between the lane markings and the highway background will not be as good.

The test arrangement for reflected light studies is shown by the illustration in **Figure 4.12**. A large black baffle with a 2" cut out is attached to the lamphouse. The cutout is centered on the lane target. A Leica projection lamp front-illuminates a 5" diameter spot on this baffle. The beam is initially centered on the target. During the experiment, the lamphouse will be moved laterally several centimeters **but the target will always remain inside the illuminated spot.** For this experiment, the lamp in the lamphouse will not be used. The target has been modified by backing it with a white card. The lane lines will be seen not by transmitted light as before but by light scattered from the white card located behind the lane slits. This test arrangement should closely approximate a road condition where fresh white lane line paint resides on fresh black macadam, and where the roadway is illuminated by the sun on a clear day.

Figure 4.13 shows the images formed by the cylindrical lens when the target is centered on the Leica beam footprint, and when it is shifted to either side (3 & 4 cm respectively). Note that the lane image shifts relative to a stationary background (which appears uniform).

4.5 Lab I Reflected Light Test Results

Figure 4.14 shows a PHR detector scan for the case shown in **Figure 4.13(b)**. The signal from the lane lines is quite strong, and resides on a uniform background plateau whose strength is less than 20% that of the line signal.

(a)   (b)

Figure 4.12 Lab I modified for reflected light tests.
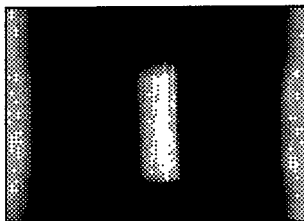
(a)   (b)   (c)

Figure 4.13 Photographs of reflected light lane image as a function of lateral offset of lamphouse.
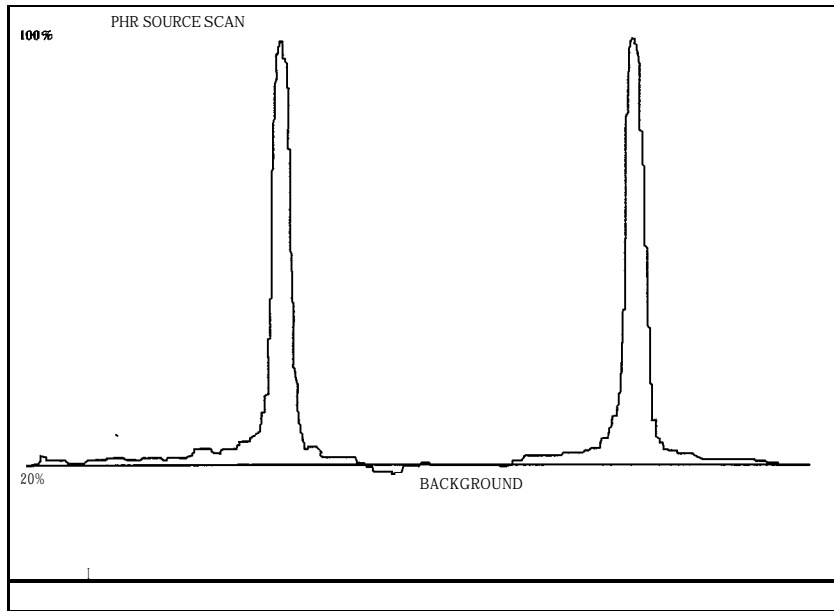
Figure 4.14 PHR detector scan of lane image formed in reflected light

Figure 4.15 shows the PSD source scan, i.e. a plot of the voltage signal from the stationary PSD as the lamphouse is moved over a range of 7 cm. The important point **is** that the lane image shift against a stationary background signal is clearly seen in reflected (or scattered) light,
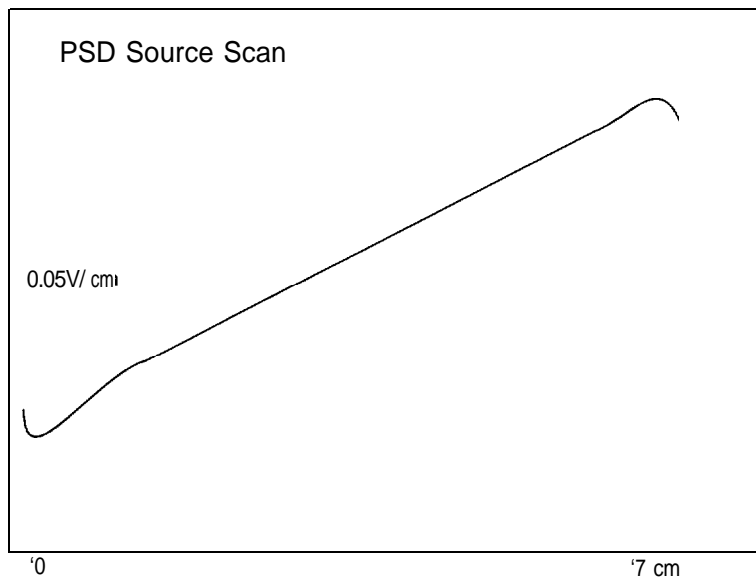
Figure 4.15 PSD source scan of lane image in reflected light.

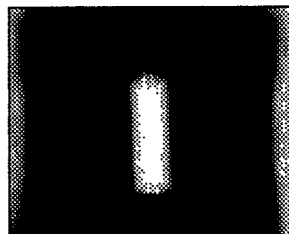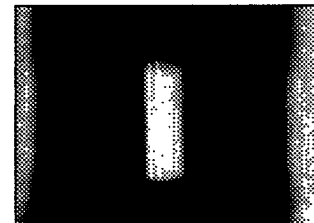The experimental setup used in the previous section lends itself to answering another question. What happens to the characteristic PSD curve when one lane line is white and the other yellow (as occurs on real roadways)? Using actual yellow road paint, the white card behind the right lane slit (when facing the target) was painted yellow. The effect on the characteristic curve is shown in **Figure 4.16.** The letters "W-W' indicate that both lane lines are white. The letters 'W-Y' indicate a mixed color lane. We do see a slight change in slope. The hybrid lane is a bit shallower.

15
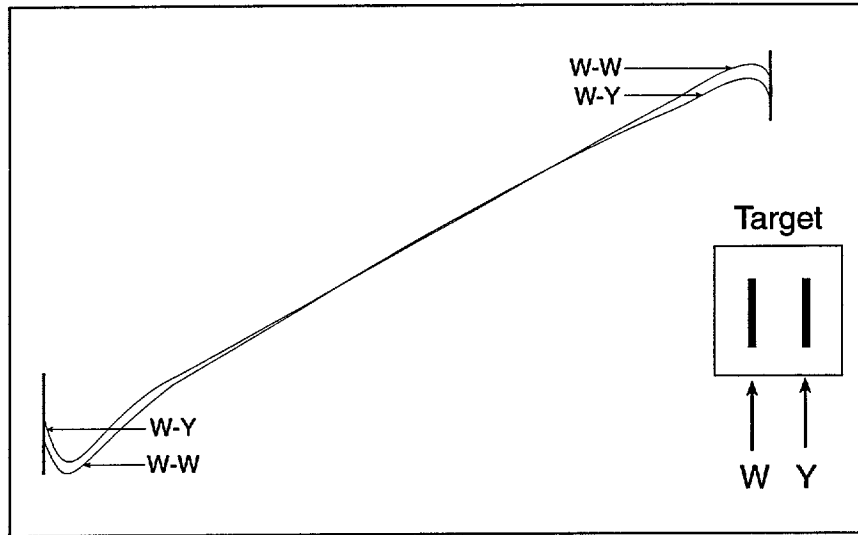
Figure 4.16 PSD source scan in reflected light showing the effect of a lane line color change.

4.6. Lab II Test Configuration

All experimental PSD and PHR scans (and lane image photographs) thus far have made use of the test configuration shown in Figure 4.1. In this configuration the planes containing the target and the cylindrical lens are parallel with each other. This will not be the operational scenario for a vehicle-mounted LPM. These planes will be tilted with respect to each other in both azimuth and elevation. To simulate this geometry the test arrangement shown in **Figure 4.17** was utilized.
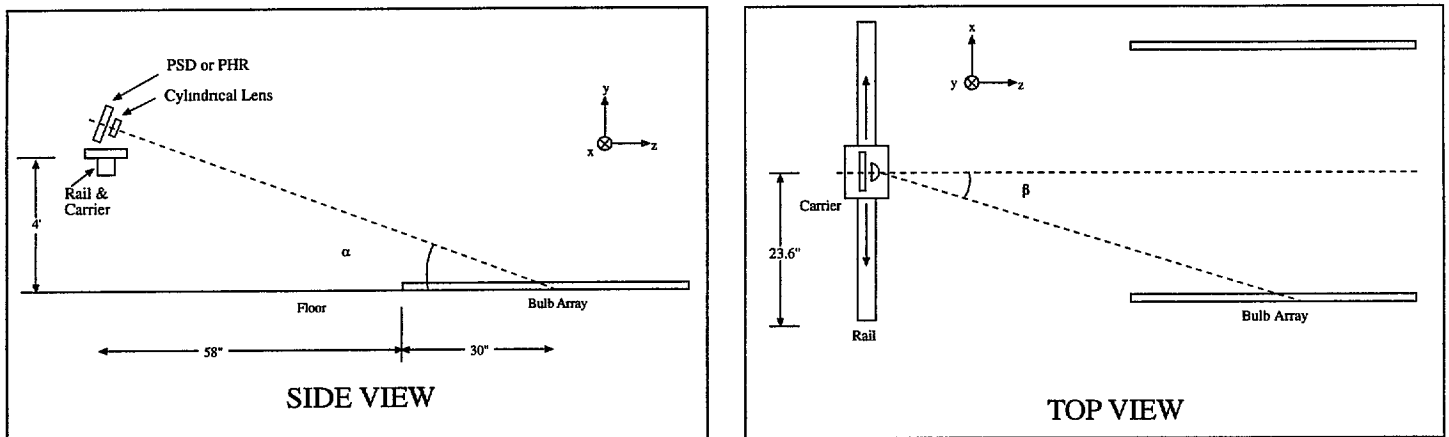
Figure 4.17 Lab II test configuration.

Here the "source" was two parallel line bulb arrays lying on the lab floor to simulate a lane. Each line bulb array consisted of white Xmas tree lights taped to 1" x 2" boards 65.5" long. They are laterally separated by 36" (91.4 cm). The boards are painted flat black. Black diffuse paper was used as a background to improve contrast. Room lights were on over the operator area but not over the bulb array.

16

The test stand consists of a 2 meter optical rail supported between two tripods. A carrier is attached to the rail and can translate along the rail. The motion of the carrier is motor driven. A Black & Decker battery powered screwdriver handle is attached to the rail at one end. It is connected via thin metal cables and pulleys to the carrier. Pressing the switch on the power handle can move the carrier right or left (depending on switch position). The motion of the carrier is smooth and fairly uniform. (However, when much of the battery energy has been consumed, the velocity of the carrier is noticeably slower.)

Attached to the carrier is a stacked sensor array (shown in **Figure 4.18).** The sensor array is connected to the carrier via a hinge whose angle can be adjusted. This allows the lane lines to be viewed at an optimum angle. These sensors include a position sensitive detector (PSD), a pinhole radiometer (PI-R), and a direct view system. All are packaged within similar containers and have identical cylindrical input optics (25 mm x 6 mm, 6.33 mm focal length lenses). The direct view system is a low power magnifier with a scaled reticle in its object plane. The image formed by the cylindrical lens is located in this same object plane. This allows the observer to see an image identical to those formed on the PSD chip and pinhole plane. The pinhole radiometer is a bit different this time. The sensor head is a 100 micron pinhole with a fiber optic cable behind it. The output end of the cable is attached to the detector head residing at an another location.
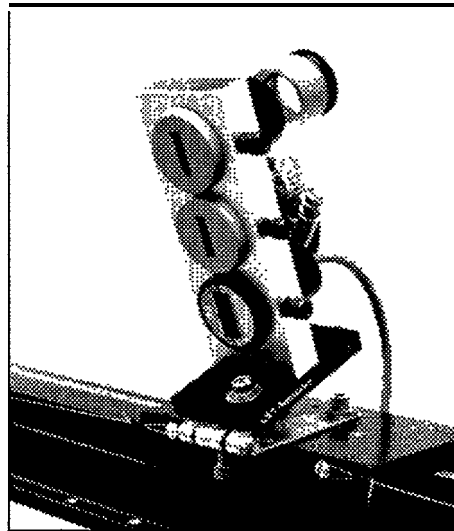
Figure 4.18 Photograph of **Lab II stacked** sensor **array.**

4.7 Lab II Test Results

When the carrier was centered in the lane, the lane image was 2.1 mm wide as seen through the direct view. The right or left line image would be sharpest when the carrier was directly over that line. As the carrier moved laterally away from that position, the line image blurred out (i.e. width increased and intensity dropped). The amount of blur was proportional to the lateral offset of the carrier. Consequently, when one lane line is sharp the other is significantly blurred.

This lateral blur of a line image is not due to lens aberration but rather to the first order imaging properties of the lens. This is made more obvious when only three bulbs in a lane line are imaged (one bulb at each end of the array and one in the middle). Then three distinct line images are seen..one for each bulb. They

are displaced laterally and vertically from each other. The vertical displacement depends on the bulb location along the Z-axis. There is lateral displacement because each bulb (although at the same X-axis location) is at a different field angle position relative to the lens (again because of Z-axis location). However, the PSD is not affected by blur width but by its centroid location. Consequently, the separation between lane line centroids is constant regardless of carrier location.

Figure 4.19 is a composite of the PHR and PSD scans. The total length of the scan is 120 cm (which is wider than the lane width), and the time base is 10 mm/sec. The sensor array declination is 21". The PHR scan shows a high contrast (0.89) lane signal. The PSD scan is very linear.
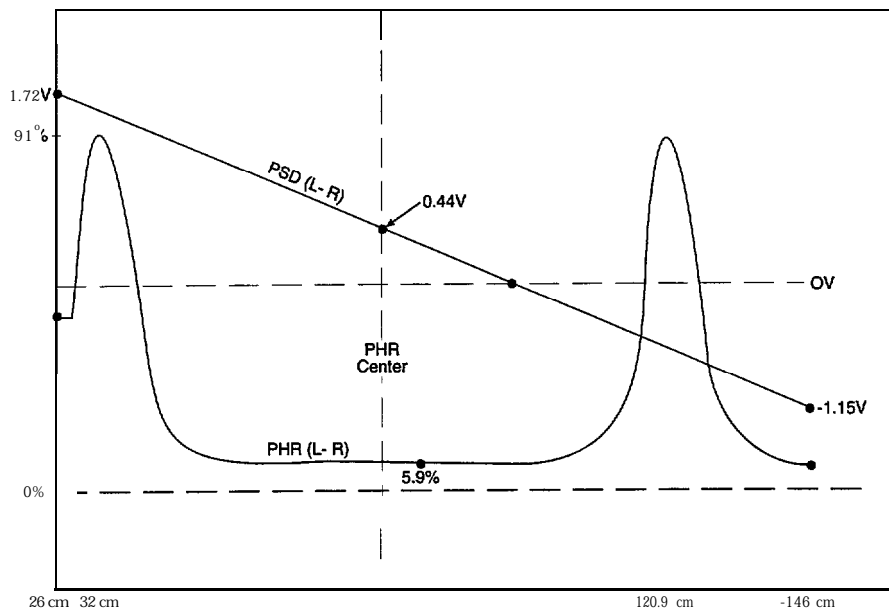

Figure 4.19 Overlay of PSD and PHR scans for Lab II configuration.

Ideally, if the only light incident on the PSD chip consists of two equally intense lane lines plus a constant background, then a zero voltage signal would indicate that the lane is perfectly centered on the chip. Note, however, that the PSD crosses the PHR centroid at +0.44 V. This may be partially explained by the fact that the left bulb array had 49 sources instead of 48. In addition, bulb intensities varied enough to be noticeable. Finally, any stray sources of reflected light (also imaged as lines) could introduce a centroid bias (although this is not evident from the PHR scan).

4.8 Field I Test Arrangement

The Lab II tests confirmed the basic operation of the motorized carrier and the stacked sensor array. However, moving this setup outside posed one major problem . . . electrical power. All the sensor heads needed it. Indoors, the sensors ran off of wall AC. An extension cord several hundred feet long for use outside was impractical. The solution was a DC to AC power inverter connected to a 12 volt battery. This provided power for the X-Y chart recorder, radiometer, and the PSD amplifier. All this equipment was loaded on a tri-level cart. A photograph of the field test setup is shown in **Figure 4.20.**

18
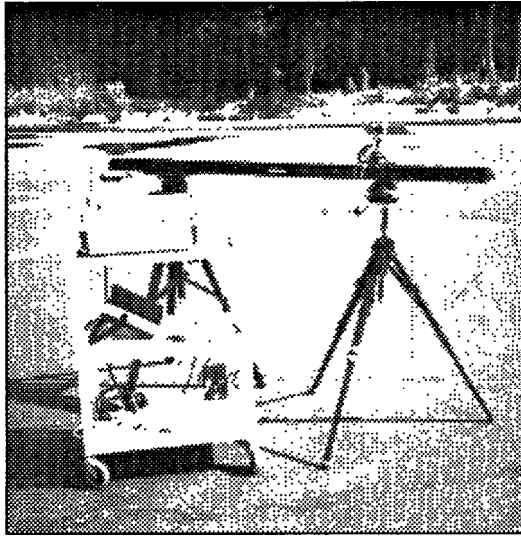
Figure 4.20 Field I testing arrangement

The test lane width in the parking lot was 55" (139.7 cm). The width of each line was 4" (10 cm). This allowed the sensor array to be scanned across the entire lane with some room to spare. [Note: The normal width of a parking space in our lot is 107" (271.8 cm), but the rail is only 200 cm long.]

4.9   Field I Test Results

4.9.1 Results 1

Figure 4.21 shows a composite of PHR and PSD scans. The mid- October day was bright and sunny with no clouds. The scans were made around 1:30 PM. The contrast between the lane lines and the background in reflected sunlight was 0.57. This is lower than in the lab test discussed above but still decent. The scan length was about 163 cm. The sensor declination was 21°.
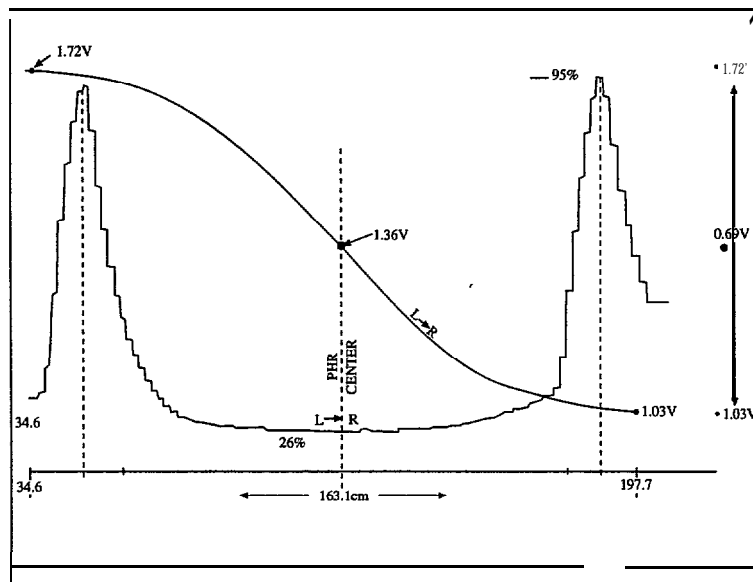
Figure 4.21 Composite PHR and PSD scan from initial field test.

19

The PSD scan is not as linear as in the lab test but we are covering about 36% more range. The scan is monotonic, smooth, and the central 50% of the plot is fairly linear. Note that the PSD voltage when the lane is physically centered on the chip is +1.36 V instead of zero. This means that the overall background light on the chip is nonuniform and is providing a bias offset. This light is from extraneous external sources in the field of view.

4.9.2 Results 2

This was a series of seven separate tests conducted over a continuous 10 hour period to examine sensor behavior for a diverse set of lighting conditions. The day was clear with occasional high wispy clouds. The first data set was collected at 9:15 AM while the test area was still in shadow. (The Sun was still below a tree line located behind the sensor array). The last test was conducted in the dark at 7:15 PM. The test area (lane lines) was illuminated by car headlights projecting light from behind and below the sensor array. **Figure 4.22** illustrates the test setup relative to the Sun's location. Elevation and azimuth angles (in degrees) are tabulated in Table 4.2. The sensor head declination was 27°.
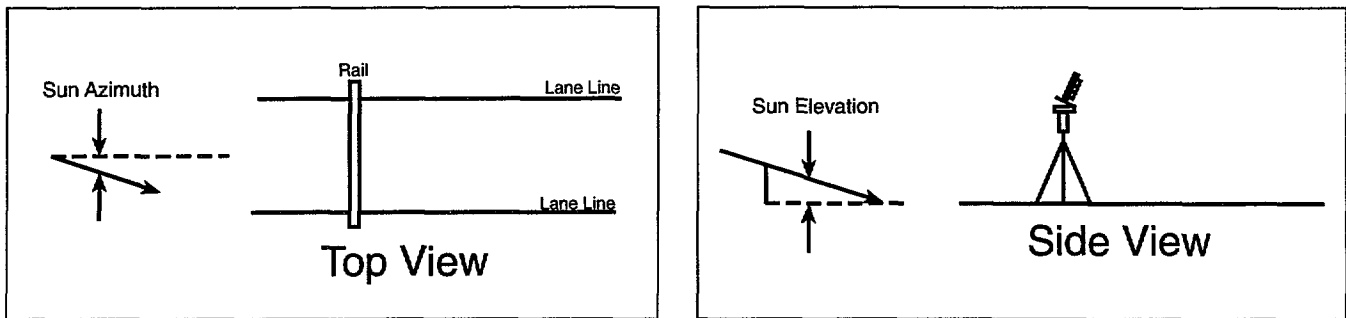
Figure 4.22 Orientation of second field test relative to Sun angle.

TABLE 4.2

Time	Azimuth	Elevation
9:15 AM	................................(in shadow)............................	
10:30	+4.5	31.4
12:55 PM	-37.2	40.3
2:30	-67.8	34.8
4:30	-94.0	17.0
6:00	............................(dusk...Sun set)...........................	
7:15	................................(Headlights)............................	

Because of the continuously changing lighting conditions, the gain setting on the 301-DIV PSD amplifiers were sometimes changed (on the last two data sets). There were also scale changes on the Y-axis of the chart recorder to accommodate the pen swing. The time base on the recorder was constant at 5 mm/sec. The speed of the carrier varied slightly from test to test depending on the charge remaining on the power handle. (Usually, the handle was brought in the lab and placed on

20

its charger between tests). For the PHR scans only data sets 3-5 can be compared directly from the plots because there was no renormalization, i.e. resetting the 100% level, between them.

Figure 4.23 is an ensemble of all seven PSD scans. Indicated on each scan are the test number, time of day, gain setting on the 301-DIV, and Y-axis scale setting. Note that tests 3-5 have the same settings. Although the starting position on the rail was the same for all tests, end-points varied (due to variations in carriage speed). Nonetheless, all scans are roughly the same length (at about 160 cm). The main point of these tests was to see if linear PSD scans could be obtained as reflected light levels waxed and waned. The data indicates that this was so.
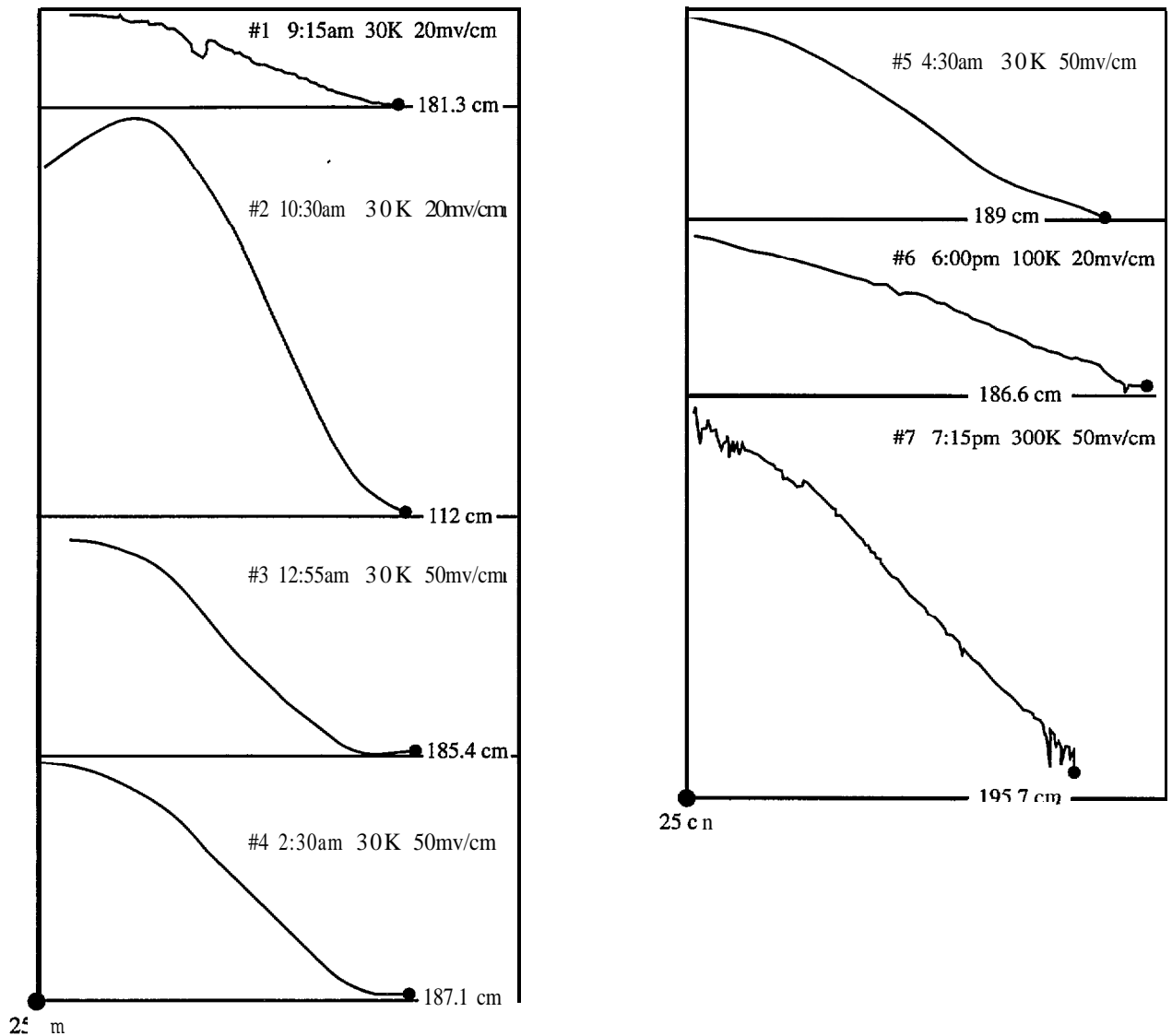
Figure 4.23 Montage of seven PSD scans obtained during course of the day.

Test 1 shows an irregular region about a third of the way into the scan. This was due to two cars which crossed the sensor FOV during the scan. They were about 80 feet in front of the array. Test 7 was the only scan with obvious noise on it. It also had the highest gain setting. Nonetheless, it still has a nice linear region.

21

The voltage readings out of the 301-DIV were monitored for all tests. Plotted in **Figure 4.24 are the** beginning and end voltages for each PSD scan. Note that l-5 have the same gain setting. Ideally, all boxes should be vertically centered on zero volts. This is because a uniform background illumination should have no effect on the position signal of the lane. But remember that we were in a parking lot. Although the area immediately around the test area was clear and dominated by high contrast lane lines, other objects were also in the field of view particularly cars. Further, the number, arrangement, and lighting of these objects changed during the course of the day. This means a nonuniform and varying background on the PSD chip which induces a positional offset bias on the PSD signal.
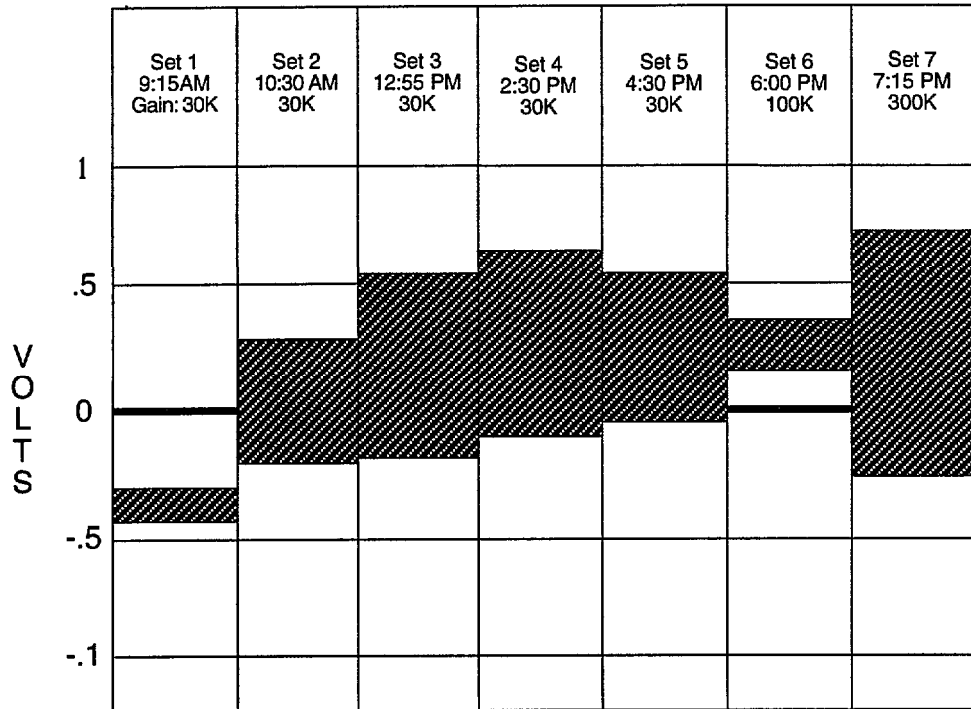
Figure 4.24 High and low voltage readings from 301-DIV
at the beginning and end of the PSD scan.

Note that, as the day progresses, the swing on the position signal increases (for a fixed range of carriage motion). At 9:15 the swing is fairly narrow. Between noon and 3 PM the size of the swing is maximum and also stable. It contracts again at 4:30 PM (as the Sun starts going down). Theoretically, position is normalized against input power. This would mean that the PSD signal swing should remain constant. Obviously this isn't so, and does not agree with what was found in Section 4.3.5. During the day, the illumination on the target area (and hence the irradiance on the chip) is changing significantly. Perhaps detector threshold effects at the lower light levels are the culprit. This will need further investigation.

A comparison of PHR scans 3-5 is presented in **Figure 4.25.** All scans start at the 25 cm mark on the rail. Ideally, the line images should be centered relative to one another. The left lane lines match up reasonably well. However, the right lane lines are staggered. Unfortunately, this is due to speed

variation in the power handle (which is affected by charge drain). As the day wears on from about 1 to 4:30 PM, the decreasing illumination is evident in the lane line and background signal levels.
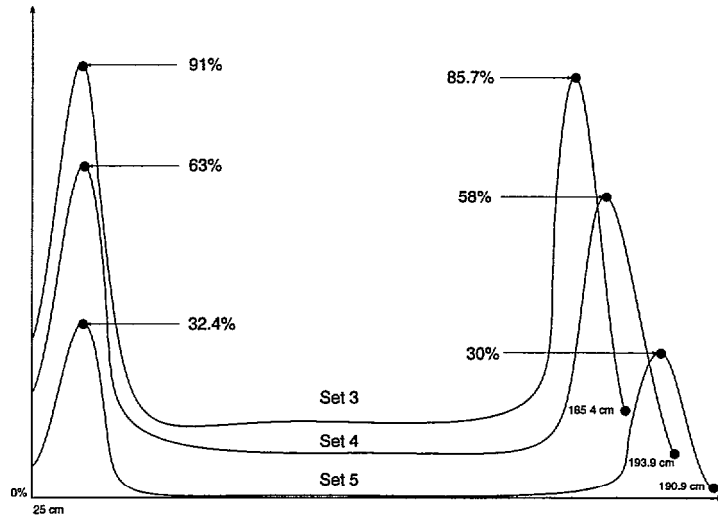

Figure 4.25 Comparison of PHR scans 3 through 5.

Figure 4.26 is a composite of the PSD and PHR scan for data set 4. There is a nice long linear region in the central portion of the PSD plot. The slope of the curve is flatter when the carrier is directly over the lane lines.
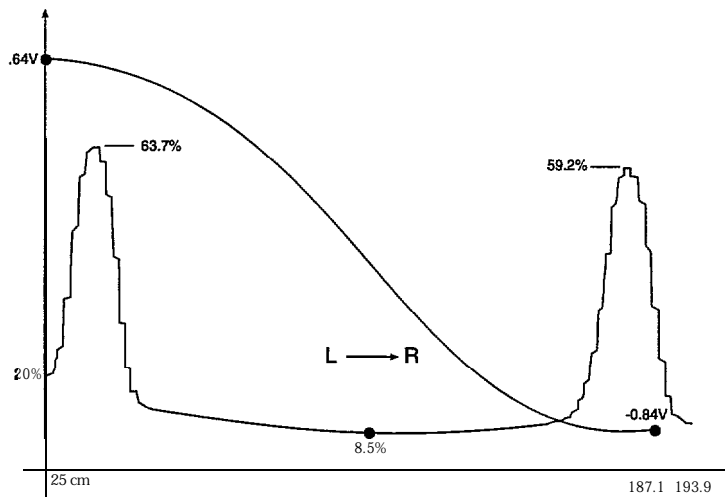

Figure 4.26 Composite PSD and PHR scan for test #4.

4.10 Field II Test Setup & Results

The Field II vehicle tests were a modest extension of the Field I experiments. The primary goal was to demonstrate a practical mating of the hardware to a real vehicle, and to take some preliminary data in our

parking lot. (Actual road tests were never envisioned within the context of this contract.) The sensor array used in the Lab II and Field I test configurations was attached to the hood of a Minivan as shown in **Figure 4.27 (a).** Only the PSD and direct view elements were used for these tests. The test equipment located inside the vehicle is shown in **Figure 4.27 (b).** Power for the PSD system was provided by an inverter connected to the vehicle's cigarette lighter. A voltmeter was used to read the position signal from the 301-DIV amplifier.


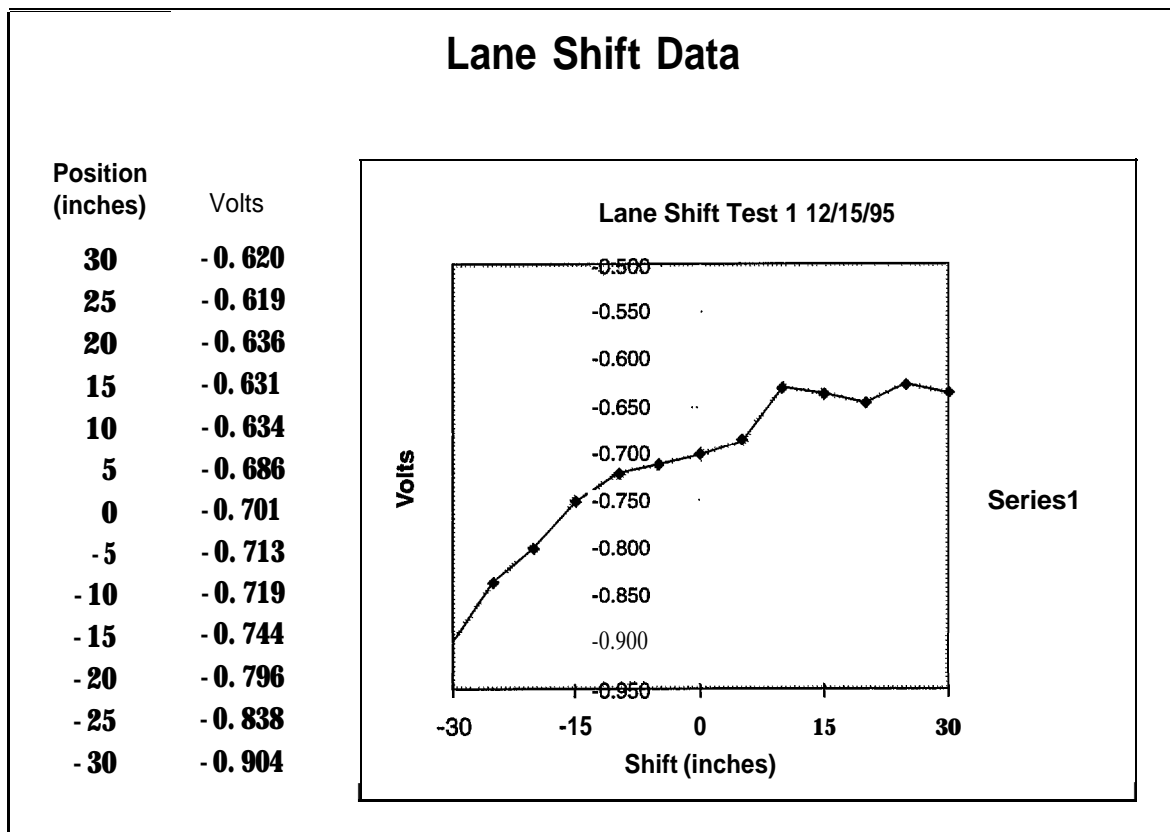**Figure 4.27   (a) Sensor array attached to hood of Minivan**

Figure 4.27 (b) Test equipment inside van

The original test plan involved jockeying the Van until it was lined up parallel to the lane at some maximum lateral offset. A reading would be taken with the Van stationary. The process would be repeated at a different but smaller offset. This would continue until data for the complete PSD curve had been collected. In practice this test procedure proved impractical. Aligning the Van parallel to the lane with monotonic offsets was extremely difficult and time consuming. An alternate approach was adopted. The Van would remain stationary while a lane target was shifted laterally relative to the Van. The lane target was a 4' X 10' piece of cardboard painted black with a 36" wide lane whose lines were formed from white tape. This target is shown in **Figure** 4.28. The lane target lateral position was measured from the center of the Van to the center of the lane using a tape measurer.
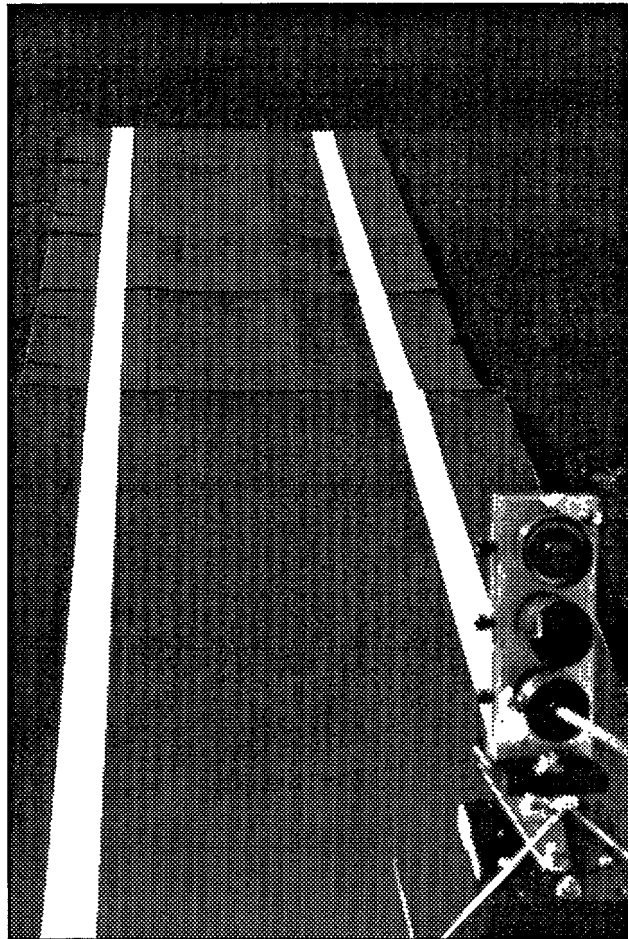
Figure 4.28 Cardboard lane target used for vehicle mounted LPM test

Unfortunately, there is not a lot of vehicle test data. The weather between early December and mid-January (the end of the contract) was poor (cloudy, freezing, or wet). The few sunny days available were very cold. (We did not want to risk damaging our PSD lab equipment.) The ice storm in December and the "Blizzard of 96" in January also thwarted outdoor tests. The only data collected is a single practice test conducted on December 15. The results are plotted in **Figure 4.29.**

Lane Shift Data

Position (inches)	Volts
30	- 0. 620
25	- 0. 619
20	- 0. 636
15	- 0. 631
10	- 0. 634
5	- 0. 686
0	- 0. 701
-5	- 0. 713
-10	- 0. 719
-15	- 0. 744
-20	- 0. 796
-25	- 0. 838
-30	- 0. 904

Lane Shift Test 1 12/15/95

Volts vs Shift (inches), Series1

**Figure 4.29 PSD plot from practice test on Minivan**

Although the signal is monotonic with position, the plot in **Figure** 4.29 is not considered good data. Part of the problem was variable illumination on the target due to clouds moving pass the Sun. This may be related to the problem seen in Figure 4.24. There the illumination was constant during a test but varied between tests. We believe good linear data could have been achieved had weather and time permitted.

5. PLANS FOR IMPLEMENTATION

Swales and Associates will actively seek a sponsor or partner to continue these investigations with the goal of developing and building a vehicle prototype. A mockup of such a prototype has been built. Photographs of the mockup are shown in **Figure 5.1** by itself **(a)** and attached to a windshield **(b).** The amplifier and display package (including a warning alarm) would most likely be mounted on (or in) the dashboard.
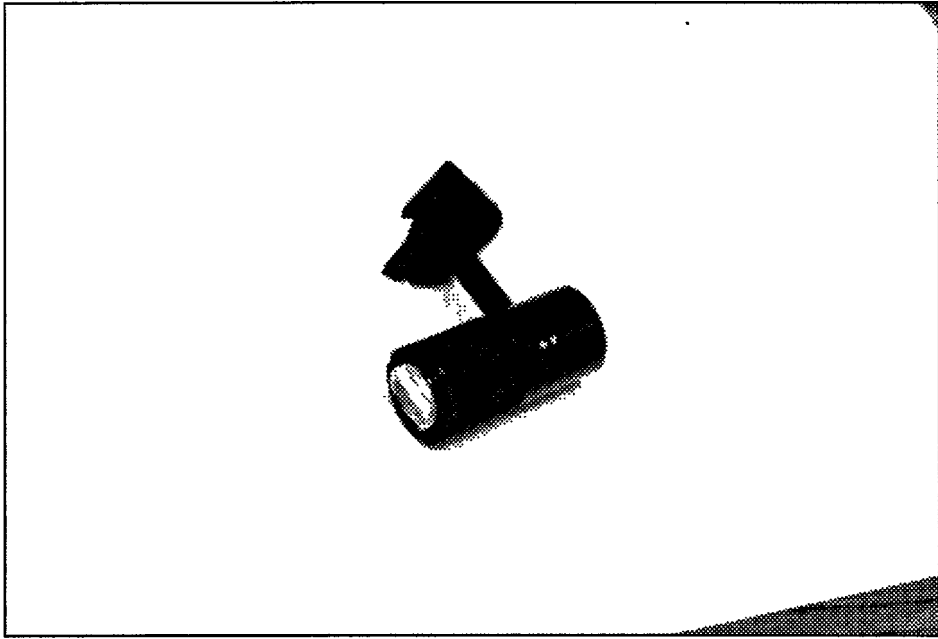
(a)
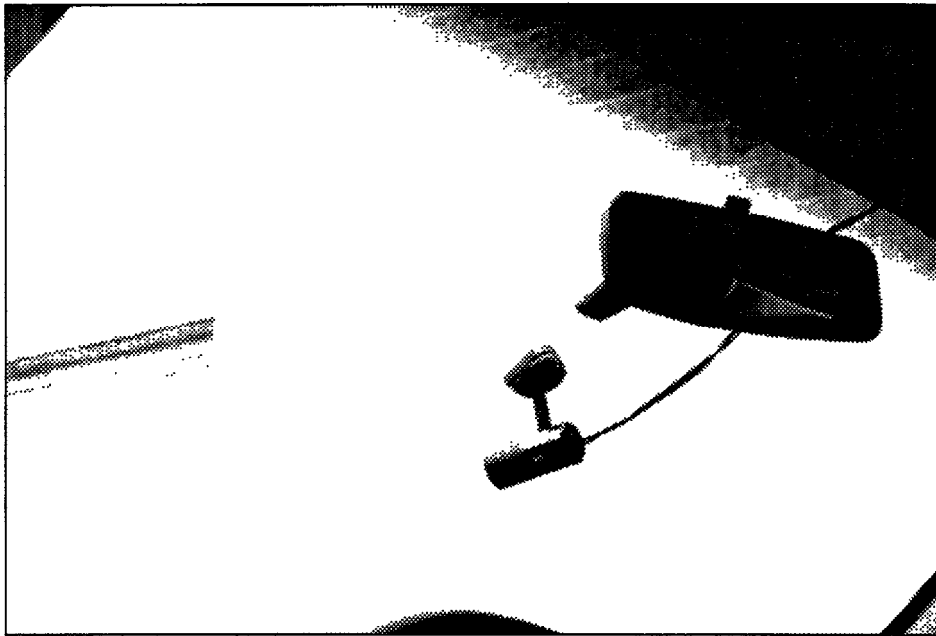
(b)

Figure 5.1 LMP mock up

6. CONCLUSIONS

This IDEA project has successfully demonstrated the feasibility of a novel passive optical LPM based on cylindrical optics and position sensitive detectors. There appear to be no insurmountable technical issues at this point. This sensor represents a new and different way of locating a vehicle's position within a lane. Since it is a new technique, everything in this report expands the transportation practice knowledge base.

The test results in this report are encouraging. First, there is sufficient contrast between the lane lines and macadam

background via reflected sunlight throughout the day to provide a decent signal to noise. Second, at night there is sufficient illumination provided by headlights to provide enough signal for the PSD. Third, there is significant linearity in the PSD response at all light levels. Fourth, the location of the vehicle in the lane is obtained in a simple straight-forward manner by a simple analog signal. No sophisticated computer/software is needed to do this. Fifth, except for baffling, the PSD sensor head employed here is close to what might be used in real life.

Much work remains, especially vehicle tests, that will further define and refine the sensors operational envelope. For this a vehicle prototype must be designed, built, and installed aboard a mobile testbed. In addition, production costs for a mass produced LPM based on the prototype need to be refined. A mass produced LPM would not use the 2 dimensional PSD employed in the laboratory and field experiments discussed here. Instead, a one dimensional linear PSD would be utilized. Preliminary estimates from Graseby Optronics for such a detector (in lots of 10,000) are $80-$100. Graseby envisions redesigning the amplifier for production units which should lower costs as well as make a smaller package. However, at the present time they can only estimate costs for their baseline 301-DIV unit. This is approximately $225/unit. Costs for the cylindrical lens were obtained from Melles-Griot. They estimate $10/lens. No costs associated with the packaging and assembly of the LPM have been obtained as yet. This will depend on the future prototype design for vehicular experiments.

7. INVESTIGATOR PROFILE

The Principal Investigator on this project was Dr.Joseph Geary. DrGeary holds an MS and PhD in optics from the University of Arizona's Optical Sciences Center. Dr. Geary has worked in the field of optics for 29 years in such diverse areas as aerial reconnaissance, medical optics, high energy lasers, optical metrology, and spaceborne optical systems. He is currently manager of the Swales' Optics Group. He has written over 40 papers for refereed journals, and is author of the books "Introduction to Optical Testing", and "Introduction to Wavefront Sensors". Dr.Geary holds 10 patents. The work for this project was conducted in the Swales optical laboratories. These are well equipped facilities which have in the past supported such diverse tasks as: proof-of-concept demonstrations; experimental investigations; and optical metrology prototype instrument building.

8. ACKNOWLEDGEMENTS